



Journal of Advanced Research in Fluid Mechanics and Thermal Sciences

Journal homepage:
https://semarakilmu.com.my/journals/index.php/fluid_mechanics_thermal_sciences/index
ISSN: 2289-7879



Natural Convection in a Spherical Porous Annulus with Diathermal Partition Wall

Sangita^{1,*}

¹ Bhagalpur College of Engineering, Bhagalpur-813210, India

ARTICLE INFO

Article history:

Received 17 December 2023
Received in revised form 15 May 2024
Accepted 26 May 2024
Available online 15 June 2024

Keywords:

Numerical studies; natural convection; porous media; diathermal partition wall; spherical annulus

ABSTRACT

The influence of the diathermal partition wall on natural convection in a fluid-saturated porous medium has been numerically studied in the present paper. A concentric diathermal wall of infinitesimal thickness is inserted in the fluid-saturated spherical porous annulus. Due to the flow symmetry along the vertical axis, only half of the sphere is considered for simulation. A Successive Accelerated Replacement Scheme has been used to solve the Darcy flow model using the finite difference method. The average Nusselt number value decreases with the presence of a partition wall within the fluid-saturated spherical porous annulus. The percentage decrease in average Nusselt number value depends upon the position of the diathermal wall within the width of the spherical annulus. There is about a 50% reduction in the average Nusselt number with a diathermal partition wall for the cases considered in this work. The results of the present investigation will help in the proper design of porous insulation in spherical porous containers for the storage of thermal energy.

1. Introduction

In today's era, energy conservation is one of the most versatile field of research area [1]. Porous media is one by using which energy is conserved. So, it is an emerging field due to its versatile and broad application area. A few of them are listed, such as geothermal energy conversion, oil and gas lines, cryogenic containers, and thermal insulation engineering, which has attracted many researchers.

As the partition wall is inserted in the vertical enclosure, the slenderness increases, due to this the rate of heat transfer decreases when the vertical porous enclosure is much taller than wide [2]. When the vertical impermeable partition wall is inserted to separate two infinite porous reservoirs, then net heat transfer rate decreases through porous layer as shown by Bejan and Anderson [3]. Nansteel and Greif [4] investigated natural convection in a two-dimensional partial vertical divided rectangular enclosure experimentally. They found partitions suppress turbulence on vertical walls. Bejan [5] examined the effect of centrally-located internal obstructions on heat transfer through a

* Corresponding author.

E-mail address: sankum2478@gmail.com

<https://doi.org/10.37934/arfmts.118.1.132141>

two-dimensional porous layer heated from the side. Three types of flow obstruction were considered: horizontal diathermal partition, horizontal adiabatic partition and vertical diathermal partition. Bejan [5] observed that heat transfer depends upon the thermal behaviour of the partition. With a partial diathermal partition, the average Nusselt number is lower than its value for the undivided cavity in most cases. But, the use of adiabatic partition increases the heat transfer. Tong and Subramanian [6] and Beckermann *et al.*, [7] studied the natural convection in rectangular enclosures, that are vertically divided into a region filled with a fluid and another filled with a fluid-saturated porous medium. Tong and Gerner [8] stated that the placing a partition at halfway between the vertical walls of an air-filled rectangular enclosure is an effective way of reduction in heat transfer. A similar result was found by Ho and Yih [9] for a vertically partitioned cavity filled with air. Jang and Chen [10] investigated the effects of an off-centre partition and the inclination of the vertical enclosure on the natural convection heat transfer. Jang and Chen [10] concluded that average heat transfer rate depends upon the partition location. Varol *et al.*, [11] observed that heat transfer reduces in square cavity divided by an inclined plate and filled with a porous medium regardless of the position and Rayleigh number but depend upon position of plate.

Ganapathy [12] and Ganapathy and Mohan [13] studied the flow field and heat transfer induced by a temperature gradient in a hemispherical porous medium using a semi-analytical method for Brinkmann and Darcy flow model respectively.

Many researchers studied nano fluid saturated porous media without partition wall [14-21]. But, no one studied it in spherical geometry with diathermal partition wall. Also, very few literatures are available on spherical porous annulus employed with Darcy flow model, non-darcy flow model and Bossinesq approximation [22-25].

In the present investigation, a concentric diathermal wall of infinitesimal thickness is inserted in the spherical porous annulus so that one region gets divided into two sub-regions. The thermally coupled sub-regions have two different streamline flow cells, which are weaker than one streamline cell without a diathermal partition wall. A spherical porous annulus is subjected to two types of thermal boundary conditions: IHOC and ICOH. The effect of the diathermal partition wall and its position on natural convection have been numerically studied. The results of the present investigation will help, how to design porous insulation in spherical porous containers for the storage of thermal energy.

2. Mathematical Formulation

Figure 1 shows the co-ordinate system and physical configuration of a concentric spherical fluid saturated porous annulus. The inner and the outer walls of the spherical annulus are assumed to be at constant temperatures T_i and T_o respectively. T_i is greater than T_o for IHOC boundary condition and T_i is smaller than T_o for ICOH boundary condition. The symmetry surface along $\phi = 0$ and $\phi = \pi$ are treated as adiabatic.

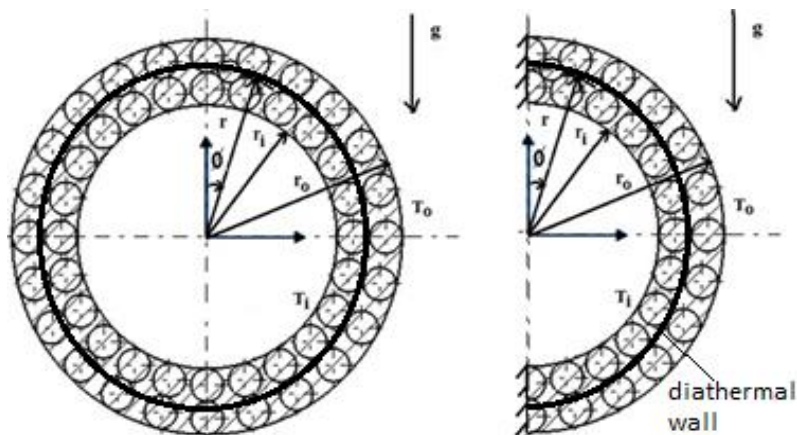


Fig. 1. Co-ordinate system and physical configuration

The flow is laminar and steady. The porous medium and convective fluid at a point is in thermal equilibrium. The governing equations for which the flow condition inside this spherical porous annulus is satisfied as follows,

Conservation of mass,

The general continuity equation for two-dimensional flow is expressed as in Nield and Bejan [26],

$$\frac{\partial}{\partial r}(r^2 u \sin\phi) + \frac{\partial}{\partial \phi}(r v \sin\phi) = 0 \quad (1)$$

Conservation of momentum [27],

$$\frac{\mu}{K} u = -\frac{\partial p}{\partial r} - \rho g \cos\phi \quad (2)$$

$$\frac{\mu}{K} v = -\frac{1}{r} \frac{\partial p}{\partial \phi} + \rho g \sin\phi \quad (3)$$

Conservation of energy,

The energy equation for isotropic porous medium without heat generation at steady state, with negligible radiative effects, viscous dissipation, and the work done by pressure changes, is given by Nield and Bejan [26] as,

$$u \frac{\partial T}{\partial r} + \frac{v}{r} \frac{\partial T}{\partial \phi} = \alpha \left(\frac{\partial^2 T}{\partial r^2} + \frac{2}{r} \frac{\partial T}{\partial r} + \frac{1}{r^2} \frac{\partial^2 T}{\partial \phi^2} + \frac{\cot\phi}{r^2} \frac{\partial T}{\partial \phi} \right) \quad (4)$$

Equation of state,

$$\rho = \rho_q [1 - \beta(T - T_q)] \quad (5)$$

These equations are solved along with following boundary conditions,

$$u = 0, T = T_i \text{ at } r = r_i \text{ for } 0 \leq \phi \leq \pi \quad (6)$$

$$u = 0, T = T_o \text{ at } r = r_o \text{ for } 0 \leq \phi \leq \pi \quad (7)$$

$$v = 0, \frac{\partial T}{\partial \phi} = 0 \text{ at } \phi = 0 \text{ for } r_i \leq r \leq r_o \quad (8)$$

$$v = 0, \frac{\partial T}{\partial \phi} = 0 \text{ at } \phi = \pi \text{ for } r_i \leq r \leq r_o \quad (9)$$

and at the partition

$$u = 0 \text{ at } r = r_f \text{ for } 0 \leq \phi \leq \pi \quad (10)$$

For inner hot and outer cold (IHOC) walls, $T_i = T_h$ and $T_o = T_c$ and for inner cold and outer hot (ICOH) walls, $T_i = T_c$ and $T_o = T_h$.

Governing equations are non-dimensional form using the following dimensionless variables,

$$R = \frac{r}{D}, \theta = \frac{T-T_c}{T_h-T_c}, U = \frac{uD}{\alpha}, V = \frac{vD}{\alpha}, \bar{\rho} = \frac{\rho}{\rho_q}, P = \frac{pK}{\mu\alpha} \quad (11)$$

In Eq. (11), $D (= r_o - r_i)$ is the gap width between inner and outer walls of spherical annulus. Stream function (ψ) is introduced such that it must satisfies continuity equation and relates velocity components U and V as,

$$U = \frac{1}{R^2 \sin \phi} \frac{\partial \psi}{\partial \phi} \quad (12)$$

$$V = -\frac{1}{R \sin \phi} \frac{\partial \psi}{\partial R} \quad (13)$$

The non-dimensional parameters, Rayleigh number (Ra), radius ratio (rr) and partition ratio (rp) are defined to solve the above equation as,

$$Ra = \frac{gK\beta(T_h-T_c)D}{\nu\alpha} \quad (14)$$

$$rr = \frac{r_o}{r_i} \quad (15)$$

$$rp = \frac{r_f - r_i}{r_o - r_i} \quad (16)$$

The extreme values of rp represents that the partition wall is at either inner surface ($rp = 0$) or outer surface ($rp = 1$) of the spherical annulus. For any intermediate position this value is less than 1. Momentum equations after elimination of pressure terms and energy equation can be expressed in terms of stream function and temperature as,

$$R^2 \frac{\partial^2 \psi}{\partial R^2} + \frac{\partial^2 \psi}{\partial \phi^2} - \cot \phi \frac{\partial \psi}{\partial \phi} = RaR^3 \sin \phi \left(\frac{\partial \theta}{\partial R} \sin \phi + \frac{\partial \theta \cos \phi}{\partial \phi R} \right) \quad (17)$$

$$R^2 \sin \phi \left(\frac{\partial^2 \theta}{\partial R^2} + \frac{2}{R} \frac{\partial \theta}{\partial R} + \frac{1}{R^2} \frac{\partial^2 \theta}{\partial \phi^2} + \frac{\cot \phi}{R^2} \frac{\partial \theta}{\partial \phi} \right) = \frac{\partial \psi}{\partial \phi} \frac{\partial \theta}{\partial R} - \frac{\partial \psi}{\partial R} \frac{\partial \theta}{\partial \phi} \quad (18)$$

Boundary conditions on stream function and temperature are given by,

$$\psi = 0, \theta = 1 \text{ (IHOC)}, \theta = 0 \text{ (ICOH)} \text{ at } R = \frac{1}{rr-1} \text{ for } 0 \leq \phi \leq \pi \quad (19)$$

$$\psi = 0, \theta = 0 \text{ (IHOC)}, \theta = 1 \text{ (ICOH)} \text{ at } R = \frac{rr}{rr-1} \text{ for } 0 \leq \phi \leq \pi \quad (20)$$

$$\psi = 0, \frac{\partial \theta}{\partial \phi} = 0 \text{ at } \phi = 0 \text{ for } \frac{1}{rr-1} \leq R \leq \frac{rr}{rr-1} \quad (21)$$

$$\psi = 0, \frac{\partial \theta}{\partial \phi} = 0 \text{ at } \phi = \pi \text{ for } \frac{1}{rr-1} \leq R \leq \frac{rr}{rr-1} \quad (22)$$

and at the partition

$$\psi = 0 \text{ at } R = rp + \frac{1}{rr+1} \text{ for } 0 \leq \phi \leq \pi \quad (23)$$

The local Nusselt number is defined as the ratio of heat flux by convection to heat flux due to pure conduction. Accordingly, local Nusselt number in non-dimensional form at the inner and outer spherical surfaces are given by,

$$Nu_i = -\frac{1}{rr} \frac{\partial \theta}{\partial R} \Big|_{R=\frac{1}{rr-1}} \quad (24)$$

$$Nu_o = -rr \frac{\partial \theta}{\partial R} \Big|_{R=\frac{rr}{rr-1}} \quad (25)$$

3. Results and Discussion

Numerical code in C++ based on successive accelerated replacement (SAR) scheme has been developed to solve the governing equations [24]. The SAR scheme is used for a set of coupled linear/non-linear second order partial differential equation with split boundary conditions. In SAR scheme, one guess profile is associated with each variable which satisfies boundary conditions. All boundary conditions are satisfied exactly at each stage of the calculation. It is natural to associate the equation for each dependent variable, which contains the highest order derivative of that variable. A numerical solution to the fully nonlinear difference equations is obtained without need to allow for the complete coupling between the equations. The ability to obtain a converged solution does not depend on the accuracy of initial guess profile. There are no as such difficulties in calculating derivative of function. SAR scheme is a point iterative and simple to develop numerical code.

Before studying model and its effects on the flow field, temperature field and the Nusselt number, parameters of SAR scheme like grid size in r and ϕ directions, acceleration factor and error tolerance have been optimised [25].

In Figure 2, a plot has been created between the Rayleigh number and the average Nusselt number at a radius ratio value of 2, in the absence of a partition wall within the spherical porous annulus, for the purpose of code validation. The present numerical code results show little deviation from the results of Burns and Tien [22] and Baytas *et al.*, [23] (past studies) due to finer mesh size and smaller value of error tolerance limit as used in the present model for radius ratio, $rr = 2$ at different Rayleigh number (Ra).

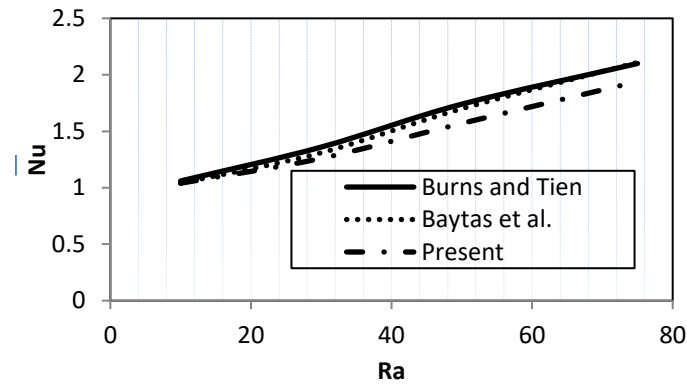


Fig. 2. Comparison of present results with the previous results in literature

Figure 3 shows streamlines and isotherms for $Ra = 1000$ at $rr = 2$. The partition wall is kept at three different positions, such as $rp = 0.25, 0.5, 0.75$. As a concentric diathermal wall of infinitesimal thickness is inserted in the spherical porous annulus, the one stronger stream flow region is divided into two different weaker convective stream flow sub-regions. But, these two sub-regions are thermally coupled due to the diathermal partition wall. Also, the isotherms are distorted less; when the partition wall is at the centre i.e., $rp = 0.5$ in comparison to the partition wall is at $rp = 0.25, 0.75$. It means that conduction is the dominant phenomenon over convection when the partition wall is at the centre. As the Nusselt number is a ratio of convective heat transfer to conductive heat transfer, the average Nusselt number decreases in this case. So, the rate of heat transfer also decreases.

Figure 4(a) and Figure 4(b) show variation of local Nusselt number with angular position when the partition ratio, $rp = 0.25, 0.5, 0.75$ at Rayleigh number, $Ra = 100$ and radius ratio, $rr = 2$ for IHOC and ICOH boundary conditions respectively. The lower value of local Nusselt number is found with partition wall as compared to without partition wall at both inner and outer wall. It is depicted from Figure 4 that the local Nusselt number value is different for different partition ratio for Rayleigh number, $Ra = 100$. This shows that position of partition wall within concentric spherical annulus plays important role for reduction of Nusselt number for Rayleigh number, $Ra = 100$ at constant radius ratio.

Figure 5(a) and Figure 5(b) show variation of local Nusselt number with angular position when the partition ratio, $rp = 0.25, 0.5, 0.75$ at radius ratio, $rr = 2$ and Rayleigh number, $Ra = 1000$ for IHOC and ICOH boundary conditions respectively. The local Nusselt number value is almost same at inner wall as well as at outer wall when the partition ratio, $rp = 0.25, 0.5, 0.75$ for Rayleigh number, $Ra = 1000$. It means the influence of position of partition wall is insignificant for higher Rayleigh number because convection dominated over conduction at high Rayleigh number. So, the position of partition wall within concentric spherical annulus is not so important at high Rayleigh number for fixed radius ratio.

Figure 6 shows variation between the ratio of average Nusselt number with partition to average Nusselt number without partition $\left(\frac{Nu_{WP}}{Nu}\right)$ by partition ratio rp for different radius ratio 1.2, 1.5 and 2 at Rayleigh number $Ra = 1000$. The plot shows that the ratio of average Nusselt number with partition to without partition is always less than or equal to one at the same Rayleigh number. This means that the heat transfer rate without partition is always more than heat transfer rate with partition. Due to the diathermal partition wall, the stronger streamline convective cell divided into two weaker streamline convective cells. The percentage of decrease in heat transfer rate depends upon the position of diathermal wall within the width of spherical annulus. The rate of heat transfer

decreases when the diathermal wall is near to inner wall of spherical porous annulus, as the radius ratio increases.

At particular value of partition ratio, there is no any effect of Rayleigh number on the ratio of average Nusselt number with partition by average Nusselt number without partition ($\frac{Nu_{WP}}{Nu}$), means it becomes constant. Figure 7 more clearly explained by Figure 5.

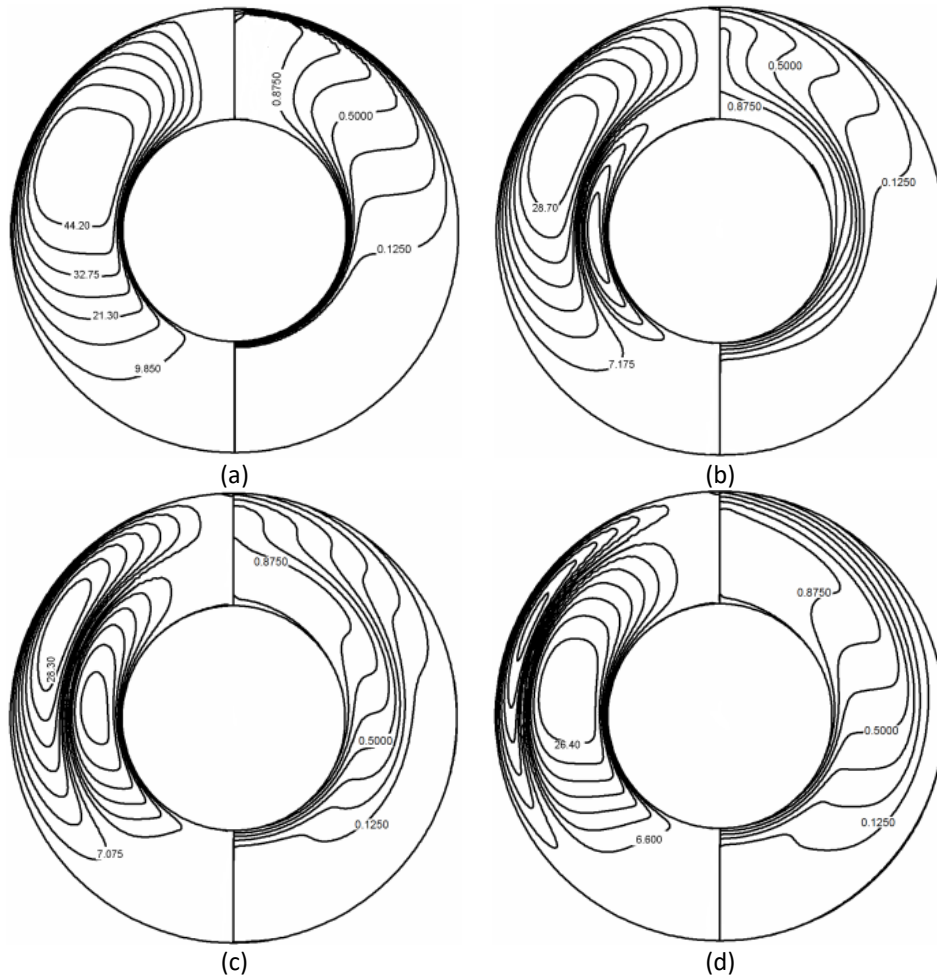


Fig. 3. Streamlines (left) and isotherms (right) for $Ra = 1000$, $rr = 2$, IHOC (a) without partition, $rp = 0$, 1 (b) $rp = 0.25$ (c) $rp = 0.5$ (d) $rp = 0.75$

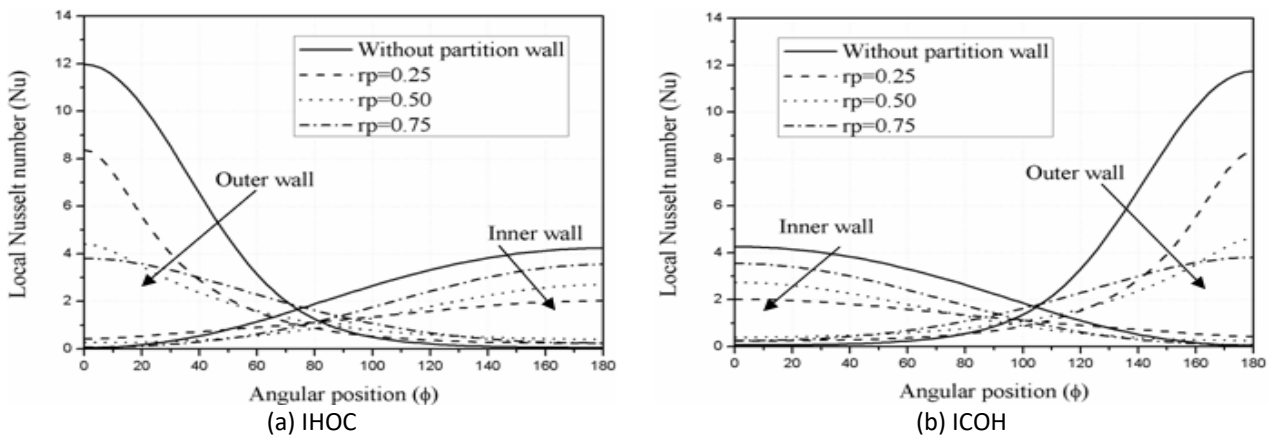


Fig. 4. Variation of local Nusselt number, Nu with angular position, ϕ (in degree) at $Ra = 100$, $rr = 2$

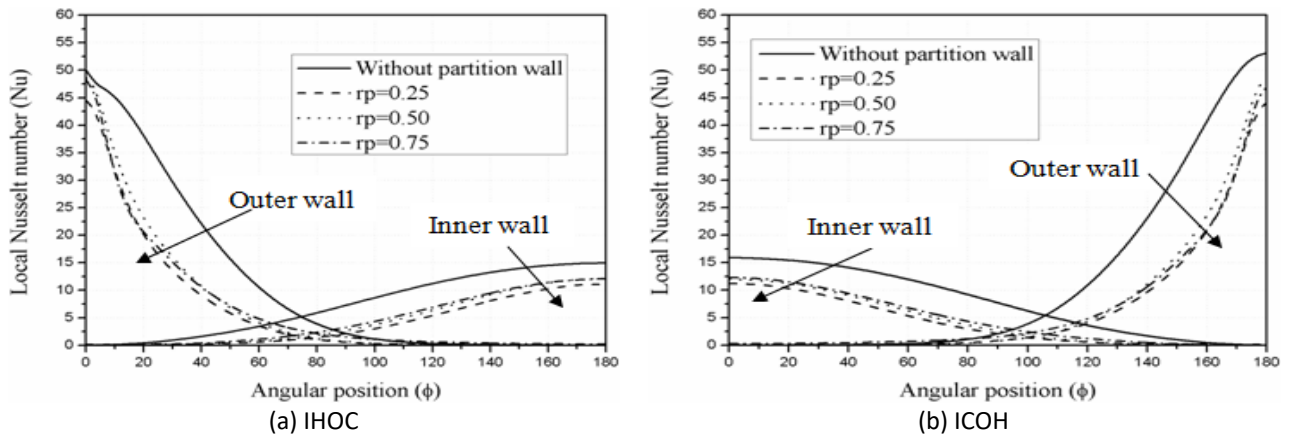


Fig. 5. Variation of local Nusselt number, Nu with angular position, ϕ (in degree) at $Ra = 1000$, $rr = 2$

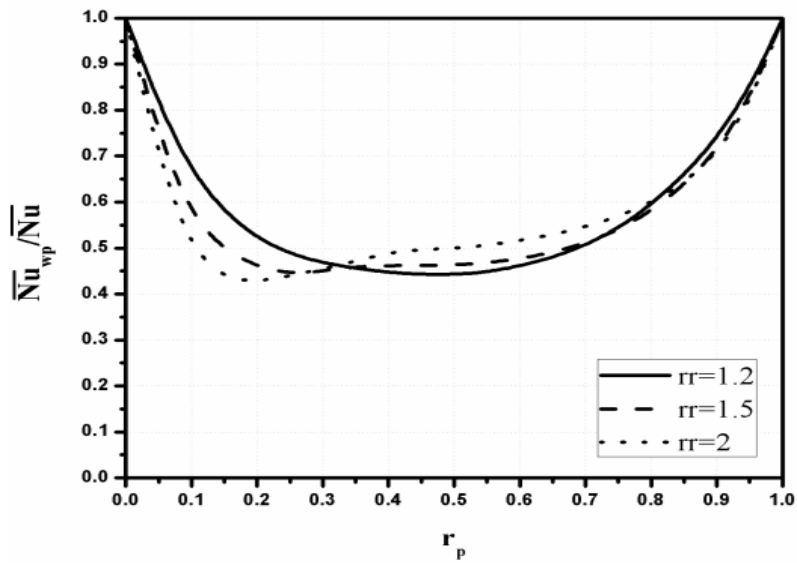


Fig. 6. Variation between the ratios of average Nusselt number with partition to without partition vs. partition ratio at $Ra = 1000$

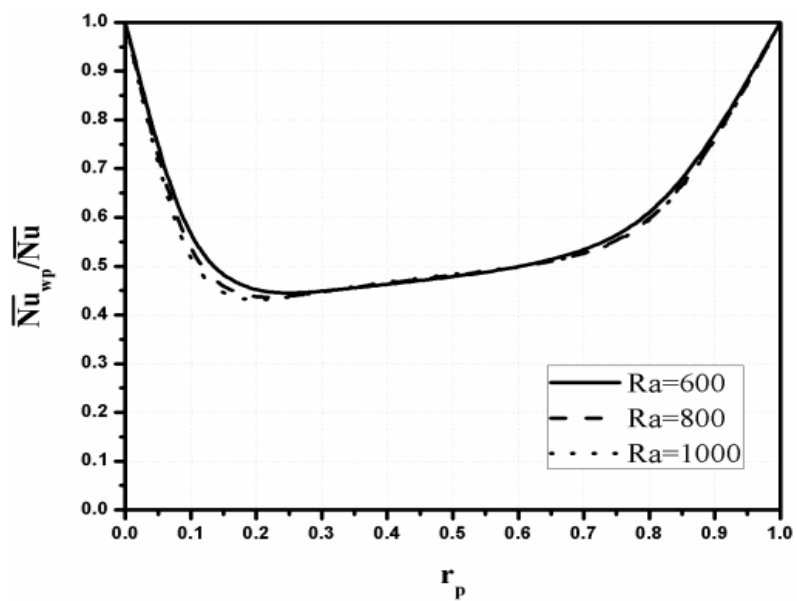


Fig. 7. Variation between the ratios of average Nusselt number with partition to without partition vs. partition ratio at $rr = 1.8$

4. Conclusions

The average Nusselt number value decreases by the presence of diathermal partition wall as compared to without diathermal partition wall within the fluid-saturated spherical porous annulus at the same Rayleigh number and radius ratio. The decrease is maximum when the diathermal wall is near to inner wall of spherical porous annulus for higher radius ratio. Due to this, reduction in heat transfer also occur. There is about 50% reduction in average Nusselt number value with inclusion of a diathermal partition wall.

Acknowledgement

This research was not funded by any grant.

References

- [1] Muhieldeen, Mohammed W., Lim Chong Lye, M. S. S. Kassim, Tey Wah Yen, and K. H. Teng. "Effect of rockwool insulation on room temperature distribution." *Journal of Advanced Research in Experimental Fluid Mechanics and Heat Transfer* 3, no. 1 (2021): 9-15.
- [2] Bejan, Adrian. "A synthesis of analytical results for natural convection heat transfer across rectangular enclosures." *International Journal of Heat and Mass Transfer* 23, no. 5 (1980): 723-726. [https://doi.org/10.1016/0017-9310\(80\)90017-4](https://doi.org/10.1016/0017-9310(80)90017-4)
- [3] Bejan, Adrian, and Ren Anderson. "Heat transfer across a vertical impermeable partition imbedded in porous medium." *International Journal of Heat and Mass Transfer* 24, no. 7 (1981): 1237-1245. [https://doi.org/10.1016/0017-9310\(81\)90173-3](https://doi.org/10.1016/0017-9310(81)90173-3)
- [4] Nansteel, M. W., and R. Greif. "Natural convection in undivided and partially divided rectangular enclosures." *ASME Journal of Heat and Mass Transfer* 103, no. 4 (1981): 623-629. <https://doi.org/10.1115/1.3244518>
- [5] Bejan, Adrian. "Natural convection heat transfer in a porous layer with internal flow obstructions." *International Journal of Heat and Mass Transfer* 26, no. 6 (1983): 815-822. [https://doi.org/10.1016/S0017-9310\(83\)80105-7](https://doi.org/10.1016/S0017-9310(83)80105-7)
- [6] Tong, T. W., and E. Subramanian. "Natural convection in rectangular enclosures partially filled with a porous medium." *International Journal of Heat and Fluid Flow* 7, no. 1 (1986): 3-10. [https://doi.org/10.1016/0142-727X\(86\)90033-0](https://doi.org/10.1016/0142-727X(86)90033-0)
- [7] Beckermann, C., S. Ramadhyani, and R. Viskanta. "Natural convection flow and heat transfer between a fluid layer and a porous layer inside a rectangular enclosure." *ASME Journal of Heat and Mass Transfer* 109, no. 2 (1987): 363-370. <https://doi.org/10.1115/1.3248089>
- [8] Tong, T. W., and F. M. Gerner. "Natural convection in partitioned air-filled rectangular enclosures." *International Communications in Heat and Mass Transfer* 13, no. 1 (1986): 99-108. [https://doi.org/10.1016/0735-1933\(86\)90076-X](https://doi.org/10.1016/0735-1933(86)90076-X)
- [9] Ho, C. J., and Y. L. Yih. "Conjugate natural convection heat transfer in an air-filled rectangular cavity." *International Communications in Heat and Mass Transfer* 14, no. 1 (1987): 91-100. [https://doi.org/10.1016/0735-1933\(87\)90011-X](https://doi.org/10.1016/0735-1933(87)90011-X)
- [10] Jang, J-Y., and C-N. Chen. "Natural convection in an inclined porous enclosure with an off-center diathermal partition." *Wärme-und Stoffübertragung* 24, no. 2 (1989): 117-123. <https://doi.org/10.1007/BF01786445>
- [11] Varol, Yasin, Hakan F. Oztop, and Ioan Pop. "Natural convection in a diagonally divided square cavity filled with a porous medium." *International Journal of Thermal Sciences* 48, no. 7 (2009): 1405-1415. <https://doi.org/10.1016/j.ijthermalsci.2008.12.015>
- [12] Ganapathy, R. "Thermal convection in a non-Darcy hemispherical porous medium." *Transport in Porous Media* 105 (2014): 105-115. <https://doi.org/10.1007/s11242-014-0362-z>
- [13] Ganapathy, R., and A. Mohan. "Free convective Darcy flow induced by a temperature gradient in a hemispherical porous medium." *Alexandria Engineering Journal* 57, no. 3 (2018): 2035-2042. <https://doi.org/10.1016/j.aej.2017.05.015>
- [14] Sankar, M., HA Kumara Swamy, Qasem Al-Mdallal, and Abderrahim Wakif. "Non-Darcy nanoliquid buoyant flow and entropy generation analysis in an inclined porous annulus: Effect of source-sink arrangement." *Alexandria Engineering Journal* 68 (2023): 239-261. <https://doi.org/10.1016/j.aej.2023.01.016>
- [15] Kanimozhi, B., M. Muthamilselvan, Qasem M. Al-Mdallal, and Bahaeldin Abdalla. "Coupled buoyancy and Marangoni convection in a hybrid nanofluid-filled cylindrical porous annulus with a circular thin baffle." *The*

- European Physical Journal Special Topics* 231, no. 13 (2022): 2645-2660. <https://doi.org/10.1140/epjs/s11734-022-00594-7>
- [16] Kanimozhi, B., M. Muthamilselvan, Qasem M. Al-Mdallal, and Bahaaeldin Abdalla. "Double-diffusive buoyancy and marangoni convection in a hybrid nanofluid filled cylindrical porous annulus." *Microgravity Science and Technology* 34, no. 2 (2022): 17. <https://doi.org/10.1007/s12217-022-09926-7>
- [17] Li, Zhixiong, Ahmad Shafee, M. Ramzan, H. B. Rokni, and Qasem M. Al-Mdallal. "Simulation of natural convection of Fe₃O₄-water ferrofluid in a circular porous cavity in the presence of a magnetic field." *The European Physical Journal Plus* 134 (2019): 1-8. <https://doi.org/10.1140/epjp/i2019-12433-5>
- [18] Li, Zhixiong, M. Ramzan, Ahmad Shafee, S. Saleem, Qasem M. Al-Mdallal, and Ali J. Chamkha. "Numerical approach for nanofluid transportation due to electric force in a porous enclosure." *Microsystem Technologies* 25 (2019): 2501-2514. <https://doi.org/10.1007/s00542-018-4153-2>
- [19] Abbas, Z., I. Mehdi, J. Hasnain, and Shaban Aly. "Role of Suction/Injection on Natural Convection Flow of Magnetite (Fe₃O₄) Nanoparticles in Vertical Porous Micro-annulus Between Two Concentric Tubes: A Purely Analytical Approach." *Arabian Journal for Science and Engineering* 44, no. 9 (2019): 8113-8122. <https://doi.org/10.1007/s13369-019-04031-1>
- [20] Mehdi, Intizar, Zaheer Abbas, and Jafar Hasnain. "Entropy generation effects with thermal radiation on MHD Casson fluid flow in porous micro-annulus." *Proceedings of the Institution of Mechanical Engineers, Part E: Journal of Process Mechanical Engineering* (2023): 09544089231189564. <https://doi.org/10.1177/09544089231189564>
- [21] Khalid, Izzati Khalidah, Nor Fadzillah Mohd Mokhtar, and Nurul Hafizah Zainal Abidin. "Thermogravitational Convection in a Controlled Rotating Darcy-Brinkman Nanofluids Layer Saturated in an Anisotropic Porous Medium Subjected to Internal Heat Source." *Journal of Advanced Research in Numerical Heat Transfer* 14, no. 1 (2023): 70-90. <https://doi.org/10.37934/arnht.14.1.7090>
- [22] Burns, P. J., and C. L. Tien. "Natural convection in porous media bounded by concentric spheres and horizontal cylinders." *International Journal of Heat and Mass Transfer* 22, no. 6 (1979): 929-939. [https://doi.org/10.1016/0017-9310\(79\)90033-4](https://doi.org/10.1016/0017-9310(79)90033-4)
- [23] Baytas, A. C., T. Grosan, and I. Pop. "Free convection in spherical annular sectors filled with a porous medium." *Transport in Porous Media* 49 (2002): 191-207. <https://doi.org/10.1023/A:1016055931290>
- [24] Sangita, Sangita, M. Sinha, and R. Sharma. "Natural Convection in a Spherical Porous Annulus: The Brinkman Extended Darcy Flow Model." *Transport in Porous Media* 100, no. 2 (2013). <https://doi.org/10.1007/s11242-013-0218-y>
- [25] Sangita, Sangita, M. K. Sinha, and R. V. Sharma. "Influence of property variation on natural convection in a gas saturated spherical porous annulus." *Transport in Porous Media* 104 (2014): 521-535. <https://doi.org/10.1007/s11242-014-0346-z>
- [26] Nield, Donald A., and Adrian Bejan. *Convection in porous media*. New York: Springer, 2013. <https://doi.org/10.1007/978-1-4614-5541-7>
- [27] Stanek, V., and J. Szekely. "Three-dimensional flow of fluids through nonuniform packed beds." *AIChE Journal* 20, no. 5 (1974): 974-980. <https://doi.org/10.1002/aic.690200519>